

Sl. No.	<p style="text-align: center;"><b>IIT Ropar</b>  <b>List of Recent Publications with Abstract</b>  <b>Coverage: May, 2020</b></p>
1.	<p><a href="#"><u>A Comparative Analysis of <math>\mu</math>PMU Placement for Active Distribution Network's Observability</u></a>  K Chauhan, R Sodhi - 8th International Conference on Power Systems, 2019</p> <p><b>Abstract:</b> Various Optimal PMU Placement (OPP) formulation have been proposed in the literature for topological observability of a power transmission system. This paper assesses the suitability of such methods for the placement of Distribution-Level Phasor Measurement Units (known as D-PMUs or <math>\mu</math>PMUs) in the active distribution network (ADN). The various OPP models such as cost minimization, channel limitation, effect of zero injection buses, single PMU loss, single line outage, multistage placement, maximization of measurement redundancy are framed and solved using Integer Linear Programming (ILP) for various ADNs such as, IEEE 33, 69 and 123 bus system. The ratio of the number of buses and <math>\mu</math>-PMUs, system measurement redundancy, depth of unobservability are considered as performance indices to compare various OPP solutions in case of normal operation, network reconfiguration and island formation.</p>
2.	<p><a href="#"><u>A Defect Estimator for Source Code: Linking Defect Reports with Programming Constructs Usage Metrics</u></a>  R Kapur, B Sodhi - ACM Transactions on Software Engineering and Methodology, 2020</p> <p><b>Abstract:</b> An important issue faced during software development is to identify defects and the properties of those defects, if found, in a given source file. Determining defectiveness of source code assumes significance due to its implications on software development and maintenance cost.</p> <p>We present a novel system to estimate the presence of defects in source code and detect attributes of the possible defects, such as the severity of defects. The salient elements of our system are: (i) a dataset of newly introduced source code metrics, called PROgramming CONstruct (PROCON) metrics, and (ii) a novel Machine-Learning (ML)-based system, called Defect Estimator for Source Code (DESCo), that makes use of PROCON dataset for predicting defectiveness in a given scenario. The dataset was created by processing 30,400+ source files written in four popular programming languages, viz., C, C++, Java, and Python. The results of our experiments show that DESCo system outperforms one of the state-of-the-art methods with an improvement of 44.9%. To verify the correctness of our system, we compared the performance of 12 different ML algorithms with 50+ different combinations of their key parameters. Our system achieves the best results with SVM technique with a mean accuracy measure of 80.8%.</p>
3.	<p><a href="#"><u>A localizing gradient damage enhancement with micromorphic stress-based anisotropic nonlocal interactions</u></a>  A Negi, S Kumar, LH Poh - International Journal for Numerical Methods in Engineering, 2020</p> <p><b>Abstract:</b> This paper presents a localizing gradient damage model with evolving micromorphic stress-based anisotropic nonlocal interactions. The objective is to model mesh independent fracture behavior of quasi-brittle materials, and to avoid the issues associated with the existing gradient enhanced damage models. In the proposed model, an evolving anisotropic nonlocal interaction domain governs the spatial diffusive behavior, which helps to maintain a localized damage bandwidth during the final stages of loading. The anisotropy in nonlocal interactions is captured through an anisotropic gradient tensor, which defines the orientation of the diffusive interaction domain based on the principal stresses at a given material point. In this paper, a smooth micromorphic stress tensor is utilized for the determination of principal stress states, to enforce a properly oriented interaction across the bandwidth of the damage process zone throughout the loading process. The proposed approach also enables the usage of low order finite elements without any oscillatory micromorphic or nonlocal equivalent strain response in the later stages of deformation. The accuracy and performance of the proposed model are demonstrated numerically in plane strain/stress for mode-I, mode-II and mixed-mode loading conditions.</p>

4.	<p><a href="#">A Novel Adaptive Droop Control Strategy for Improved Power Sharing and DC Voltage Control in MTDC grids</a> AS Kumar, BP Padhy - 8th International Conference on Power Systems, 2019</p> <p><b>Abstract:</b> In this paper a novel Adaptive Droop Control (ADC) strategy is implemented for Grid Side Voltage Source Converters (GS-VSC) of Multi-terminal HVDC (MTDC) grids. The proposed method regulated the dc voltage by sharing appropriate power between the converter stations. During any converter outage or power imbalances, the proposed ADC ensures that the rest of converters are not burdened or operated beyond the converter ratings. The proposed ADC operate effectively without any communication between the converters. The evaluation of proposed control ADC is done by creating contingencies like converter outage, fault on the AC and DC side of the grid. The proposed method shows improved performance as compared with the conventional Voltage Droop Control (VDC). The CIGRE B4 working group DC grid benchmark test system is used to show the outperform of proposed ADC scheme in comparison with conventional VDC.</p>
5.	<p><a href="#">A Review on Cellular Network Infrastructure Evolution: Challenges and Opportunities</a> SK Singh, R Singh, B Kumbhani - 14th Conference on Industrial and Information Systems, 2019</p> <p><b>Abstract:</b> Last few decades have witnessed tremendous growth in terrestrial communication. This has happened with improved technologies at both the physical layer as well as network layer level. This paper surveys some of the key technological advancements implemented towards the fulfilment of ever increasing demands. Basically, this paper provides a comprehensive review of the applications and challenges associated with different generation of communication system and technological enhancement towards their fulfilment. In addition, we discuss main features of next generation cloud radio area network architecture along with the cooperative transmission schemes. Further, it is shown that Cloud Radio Access Network (CRAN) is the most suitable alternative for next generation architecture.</p>
6.	<p><a href="#">A Semi-Intrusive Load Monitoring Approach for Demand Response Applications</a> S Dash, R Sodhi, B Sodhi - 8th International Conference on Power Systems, 2019</p> <p><b>Abstract:</b> Appliance-Load Monitoring (ALM) is essential for several demand-response (DR) programs. The techniques used for this purpose are broadly classified into two types: 1) Intrusive Load Monitoring (ILM), and 2) Non-Intrusive Load Monitoring (NILM). This paper proposes a semi-intrusive load monitoring (SILM) technique to exploit the bests of both. The method does not use any disaggregation algorithm; instead, it's an instrumentation approach to monitor the power consumption of appliances. First, it groups all appliances of a residential house in some clusters and then monitors those, in near real-time, using only one sensing-unit per cluster. A lab-scale testbed is developed to verify the claims of the proposed method. Test results demonstrate the monitoring and controlling capability and prove the cost-effectiveness of the technique. Raspberry Pi is used as the programming platform along with Python programming language.</p>
7.	<p><a href="#">Adaptive droop control strategy for autonomous power sharing and DC voltage control in wind farm-MTDC grids</a> AS Kumar, BP Padhy - IET Renewable Power Generation, 2019</p> <p><b>Abstract:</b> This study presents a novel adaptive droop control (ADC) strategy for power-sharing in a multi-terminal high-voltage DC grid while maintaining a desirable DC voltage level. The ADC scheme can share the power without burdening any power converters during one or more converter outages and huge power imbalance situations. To improve the effectiveness of the power sharing and DC voltage deviation control, the ADC is also implemented for wind farm converters. This is achieved through a derated mode operation of wind farms. The performance and effectiveness of the proposed control approach are evaluated in several case studies based</p>

	on the specific type of converter outage under the various outage scenarios. The proposed method is validated on a five-terminal CIGRE B4 DC grid test system.
8.	<p><a href="#">Algorithm and hardness result for semipaired domination in graphs</a>  MA Henning, A Pandey, V Tripathi - 17th Cologne-Twente Workshop on Graphs and Combinatorial Optimization, 2019</p> <p><b>Abstract:</b> For a graph <math>G</math> with no isolated vertices, a dominating set <math>D</math> of <math>G</math> is called a semipaired dominating set of <math>G</math> if <math>D</math> can be partitioned into 2-element subsets such that the vertices in each 2-element set are at distance at most two. The minimum cardinality of a semipaired dominating set of <math>G</math> is called the semipaired domination number of <math>G</math>, and is denoted by <math>pr_2(G)</math>. The Minimum Semipaired Domination problem is to find a semipaired dominating set of <math>G</math> of cardinality <math>pr_2(G)</math>. Given a graph <math>G</math> and a positive integer <math>k</math>, the Semipaired Domination Decision problem is to decide whether <math>G</math> has a semipaired dominating set of cardinality at most <math>k</math>. In this paper, we show that the Semipaired Domination Decision problem is NPcomplete even for split graphs, an important subclass of chordal graphs. On the positive side, we propose a linear-time algorithm to solve the Minimum Semipaired Domination problem in trees.</p>
9.	<p><a href="#">An Adaptive IIR Notch Filter based Half-Cycle P-Class Phasor Measurement Estimation Scheme</a>  Y Bansal, R Sodhi - 8th International Conference on Power Systems, 2019</p> <p><b>Abstract:</b> This paper presents a simple yet effective phasor estimation scheme, which is compliant with the protection class performance of Phasor Measurement Units (PMUs). The proposed scheme is comprised of three main steps, viz., i) real-time frequency estimation using Goertzel-Zero Crossing Detector (G-ZCD), ii) reference signal generation, and iii) fourth order Adaptive IIR Notch Filter (ANF) based phasor estimation. The proposed estimator accurately estimates the signal phasors within half a cycle of the power system frequency, and hence is suitable for P-Class PMUs development. The effectiveness of the proposed scheme is checked on different test scenarios, as per the IEEE C37.118.1a-2014 standards, confirming the potentiality of the proposed estimator to detect the possible presence of static and dynamic conditions in the signal. The validation of proposed algorithm with Real Time Digital Simulation (RTDS) data for the fault scenario in the IEEE 13 node distribution feeder integrated with Photo Voltaic (PV), is also presented.</p>
10.	<p><a href="#">An Attempt to Estimate DC Endurance Coefficient from Volume Resistivity</a>  D Sathyamoorthy, CC Reddy - 4th International Conference on Condition Assessment Techniques in Electrical Systems, 2019</p> <p><b>Abstract:</b> Ageing is a slow process of degradation of dielectric properties of cable insulation operating at high thermal stress. Prolonged thermal stress gradually weakens the insulation and ultimately leads to failure. Therefore, ageing studies are important for the design of insulation for high voltage power apparatus. One of the important properties of insulation is the resistivity of the material, especially for use in DC systems. In this paper, the authors have considered volume resistivity as a parameter to identify the changes with respect to ageing time. The ageing of insulation, change in volume resistivity and V-t characteristics are believed to be related. A batch of fresh LDPE samples was subjected to thermal stress for different time durations and the volume resistivity and permittivity of each of the samples had been measured under different electric fields. The variation in volume resistivity was analyzed experimentally and theoretically. An attempt has been made to relate endurance coefficient to changes in resistivity. Endurance coefficient has been estimated using volume resistivity.</p>
11.	<p><a href="#">Augmenting bending stroke of soft dielectric unimorph actuator using carbon nanotubes</a>  A Baranwal, P Agnihotri - Smart Materials and Structures, 2020</p> <p><b>Abstract:</b> Experimental investigations are carried out to quantify the effect of carbon nanotubes (CNTs) addition on the actuation performance of polydimethylsiloxane (PDMS) based soft dielectric elastomer actuator (DEA). The actuation ability of pure PDMS and CNT/PDMS</p>

	<p>composite samples is compared in unimorph configuration. Comparative analysis of experimental results shows that incorporation of optimum CNT concentration (0.05 wt%) significantly enhances the tip displacement (two times) and efficiency (three times) of pure PDMS based DEA. Increasing the CNT concentration beyond optimum level degrades the tip displacement and efficiency of bend actuator. The experimental results are well supported by the theoretical analysis and finite element simulations. Moreover, experimental and numerical findings are combined to establish microstructure-property relationship of DEA. It is shown that at optimum CNT concentration, the induced Maxwell stress compensates for the increase in stiffness of DEA. However, the enhanced stiffness and agglomeration beyond optimum CNT loading results in lower tip displacement.</p>
12.	<p><a href="#">BPBSAM: Body part-specific burn severity assessment model</a> J Chauhan, P Goyal - Burns, 2020</p> <p><b>Abstract:</b> Background and objective Burns are a serious health problem leading to several thousand deaths annually, and despite the growth of science and technology, automated burns diagnosis still remains a major challenge. Researchers have been exploring visual images-based automated approaches for burn diagnosis. Noting that the impact of a burn on a particular body part can be related to the skin thickness factor, we propose a deep convolutional neural network based body part-specific burns severity assessment model (BPBSAM). Method Considering skin anatomy, BPBSAM estimates burn severity using body part-specific support vector machines trained with CNN features extracted from burnt body part images. Thus BPBSAM first identifies the body part of the burn images using a convolutional neural network in training of which the challenge of limited availability of burnt body part images is successfully addressed by using available larger-size datasets of non-burn images of different body parts considered (face, hand, back, and inner forearm). We prepared a rich labelled burn images datasets: BI &amp; UBI and trained several deep learning models with existing models as pipeline for body part classification and feature extraction for severity estimation. Results The proposed novel BPBSAM method classified the severity of burn from color images of burn injury with an overall average F1 score of 77.8% and accuracy of 84.85% for the test BI dataset and 87.2% and 91.53% for the UBI dataset, respectively. For burn images body part classification, the average accuracy of around 93% is achieved, and for burn severity assessment, the proposed BPBSAM outperformed the generic method in terms of overall average accuracy by 10.61%, 4.55%, and 3.03% with pipelines ResNet50, VGG16, and VGG19, respectively. Conclusions The main contributions of this work along with burn images labelled datasets creation is that the proposed customized body part-specific burn severity assessment model can significantly improve the performance in spite of having small burn images dataset. This highly innovative customized body part-specific approach could also be used to deal with the burn region <u>segmentation</u> problem. Moreover, fine tuning on pre-trained non-burn body part images network has proven to be robust and reliable.</p>
13.	<p><a href="#">Charge-state conversion in nitrogen-vacancy centers mediated by an engineered photonic environment</a> S Sharma, RV Nair - Physical Review A, 2020</p> <p><b>Abstract:</b> The nitrogen-vacancy (NV) center in nanodiamonds has emerged as an excellent platform in quantum technologies due to its applications in spin manipulation and nanoscale sensing. However, their use is limited by the unavoidable charge-state conversion under optical pumping. In this study, we investigate the control of charge-state conversion in NV centers using an engineered photonic environment and thus change the available local density of optical states (LDOS). The spectral- and pump-dependent decay rate measurements are performed to study</p>



	<p>the redistribution of emission rates due to the change in LDOS and their effect on charge-state conversion. We have achieved an 8% enhancement of emission rate at the zero phonon line which is accompanied with a 10% suppression in the phonon sideband emission rate in the low-pump-power regime. In the high-pump-power regime, the charge-state conversion becomes inevitable and leads to the deterioration of LDOS-induced modification in the NV center emission lifetimes. The results are useful for efficient NV center spin readout and charge-state depletion microscopy utilizing reversible charge-state conversion.</p>
14.	<p><a href="#">Chemoselective Ru (II)-Catalyzed Synthesis of Aryl Thiocyanates and Step-wise Double [2+ 2+ 2] Cycloadditions to 2-Aryl Thiopyridines</a>  D Bhatt, P Kalaramna, K Kumar, A Goswami - European Journal of Organic Chemistry, 2020</p> <p><b>Abstract:</b> Ru(II)-catalyzed intermolecular double [2+2+2] cycloadditions of 1,6-diynes and alkynylthiocyanates have been developed for the synthesis of 2-aryl thiopyridines. Aryl thiocyanates were isolated chemoselectively during the course of reaction as a result of initial intermolecular [2+2+2] cycloaddition product. The method offers operational simplicity and is atom economical in nature.</p>
15.	<p><a href="#">Comparative Analysis of LMS, Block LMS and RLS Adaptive Control Methods for Shunt Voltage Source Converter</a>  B Singh, CC Reddy - 14th Conference on Industrial and Information Systems, 2019</p> <p><b>Abstract:</b> This paper gives the comparative analysis of the adaptive control mechanism which are meant for shunt connected voltage source converter (SVSC). The adaptive control mechanism driven in such a way to improve the quality of electric power under non-linear loads. The authors have implemented the three adaptive control algorithms, the adaptive control algorithm has a filtering and adaption section, the adaption section consists of least mean square (LMS), second algorithm is block LMS and then an algorithm recursive least square (RLS) finds the filter weights recursively manner. The reference current is estimate using these adaptive filter algorithms and compare with the SVSC currents to generate the required switching signals. The algorithms are compared based on several points, mainly convergence time of the weighted vectors, steady state error of the incorporated adaptive algorithm and finally the total harmonic distortion (THD) in the source current. The investigation on the algorithm are performed on the Matlab/Simulink platform under nonlinear load and dynamic load behaviour.</p>
16.	<p><a href="#">Compression and fracture behavior of leather particulate reinforced polymer composites</a>  I Surana, HS Bedi, J Bhinder, V Ghai, A Chauhan, PK Agnihotri - Materials Research Express, 2020</p> <p><b>Abstract:</b> Strategies are suggested for the waste utilization of industrial leather by preparing composites with epoxy and high-density polyethylene (HDPE). The addition of leather improves the average specific compression toughness of epoxy by 29%. The fracture surface analysis suggests the incorporation of leather microparticles leads to a transition of failure mode of epoxy from brittle to ductile. In addition, the dynamic strength of the leather/epoxy composite is found to be 69% higher than that of neat epoxy. However, no significant changes are observed when HDPE is infiltrated with leather. Apart from dispersing the leather particles directly in polymer, a novel strategy is presented here in which leather/HDPE microfibers are prepared and then used to reinforce the epoxy matrix. The specific compression modulus of this composite blend is 8% and 65% higher than epoxy and HDPE, respectively. Fractography is further carried out on the failed specimens to understand the failure mechanism in each composite. A change in the failure mode is observed when epoxy is reinforced either with leather particles or the microfiber. While the failure strength of the microfiber is found to be higher than epoxy, the strength of microfiber/epoxy interface is lower than that of epoxy.</p>

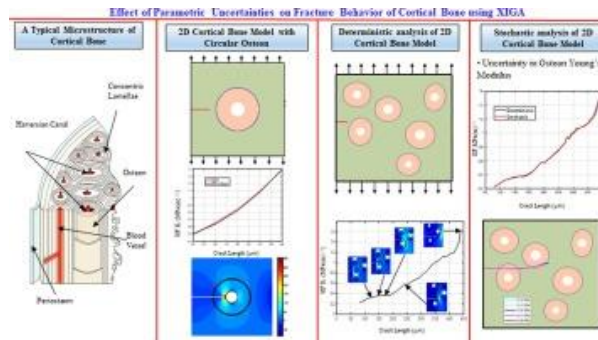
17.	<p><a href="#">Crack Propagation Behavior in Spur Gear by XFEM and Its Influence on Dynamic Characteristics</a>  JG Verma, PK Kankar, S Kumar - Reliability and Risk Assessment in Engineering: Part of the Lecture Notes in Mechanical Engineering book series , 2020</p> <p><b>Abstract:</b> This manuscript inspects the dynamic characteristics of a standard spur gear considering the effect of gear root crack and crack at pitch circle. Cracked gear pair is modeled through extended finite element method with the help of ANSYS software. This method enables the accurate approximation of solution for problems involving non-smooth features like crack within elements. Additionally, the effect of position and length of the crack on the gear structure is observed in terms of the dynamic characteristics, i.e., natural frequencies and vibration shapes. Due to the presence of crack, the natural frequency of the gear changes. These results create a worthy basis for the failure investigation and fault finding of gears.</p>
18.	<p><a href="#">Deep Underwater Image Restoration and Beyond</a>  AA Dudhane, P Hambarde, PW Patil, S Murala - IEEE Signal Processing Letters, 2020</p> <p><b>Abstract:</b> Underwater image restoration is a challenging problem due to the multiple distortions. Degradation in the information is mainly due to the 1) light scattering effect 2) wavelength dependent color attenuation and 3) object blurriness effect. In this letter, we propose a novel end-to-end deep network for underwater image restoration. The proposed network is divided into two parts viz. channel-wise color feature extraction module and dense-residual feature extraction module. A custom loss function is proposed, which preserves the structural details and generates the true edge information in the restored underwater scene. Also, to train the proposed network for underwater image enhancement, a new synthetic underwater image database is proposed. Existing synthetic underwater database images are characterized by light scattering and color attenuation distortions. However, object blurriness effect is ignored. We, on the other hand, introduced the blurring effect along with the light scattering and color attenuation distortions. The proposed network is validated for underwater image restoration task on real-world underwater images. Experimental analysis shows that the proposed network is superior than the existing state-of-the-art approaches for underwater image restoration.</p>
19.	<p><a href="#">Dependence of the far-field optical response of ion beam sculpted Cu thin films on their surface correlations</a>  Shinki, S Sarkar - Applied Surface Science, 2020</p> <p><b>Abstract:</b> Recent studies involving the properties of metallic nanostructures for potential technological applications are fundamentally rooted in their optical absorption and scattering properties. In this study, we report the far-field optical behavior of self organized copper (Cu) nanoripples on a glass substrate fabricated using low energy Ar<sup>+</sup> ion beam irradiation for varying ion fluences. The optical characterization was performed by measuring the specular as well as the diffuse component in wavelength dependent transmittance spectra for the irradiated samples. Quantitative analyses has been performed on the morphology of the nanostructured films in order to extract the surface statistical parameters like roughness, wavelength, aspect ratio and correlation length. Optical responses from the nanostructured surfaces exhibit additionally strong characteristic spectra arising out of diffuse scattering as compared to the specular ones for increasing incident ion fluences. The peak intensity and sharpness observed in the transmittance spectra was found to depend largely on the surface height correlations which showed variation with increasing ion fluences. Finally, we demonstrate the dependencies of the local surface slope and the autocorrelation function in regulation of the optical transmittance of the nanoripple structured Cu thin films.</p> <p><b>Graphical Abstract:</b></p>

20.	<p><a href="#">Discharging Characteristics of a HVDC Test-Cable</a>  A Das, CC Reddy - 14th Conference on Industrial and Information Systems, 2019</p> <p><b>Abstract:</b> In HVDC power transmission, power cables are taking the place of overhead lines at a rapid rate. While testing HVDC power cables, manufacturers often encounter difficulty of handling, as a prior knowledge of the time at which the power cable would discharge completely is not known. This paper explores the discharging time of cables of different lengths and also analyzes the factors which affect the discharging phenomenon, and tries to give a proper time after which a tested cable can be handled safely. The complexity arises because of the fact that a cable behaves as a distributed parameter transmission line. The discharging phenomenon has been simulated using PSPICE software and also some of the results are verified analytically.</p>
21.	<p><a href="#">Duality and transport for supersymmetric graphene from the hemisphere partition function</a>  R Gupta, C Herzog, I Jeon - Journal of High Energy Physics, 2020</p> <p><b>Abstract:</b> We use localization to compute the partition function of a four dimensional, supersymmetric, abelian gauge theory on a hemisphere coupled to charged matter on the boundary. Our theory has eight real supercharges in the bulk of which four are broken by the presence of the boundary. The main result is that the partition function is identical to that of <math>N = 2</math> abelian Chern-Simons theory on a three-sphere coupled to chiral multiplets, but where the quantized Chern-Simons level is replaced by an arbitrary complexified gauge coupling <math>\tau</math>. The localization reduces the path integral to a single ordinary integral over a real variable. This integral in turn allows us to calculate the scaling dimensions of certain protected operators and two-point functions of abelian symmetry currents at arbitrary values of <math>\tau</math>. Because the underlying theory has conformal symmetry, the current two-point functions tell us the zero temperature conductivity of the Lorentzian versions of these theories at any value of the coupling. We comment on S-dualities which relate different theories of supersymmetric graphene. We identify a couple of self-dual theories for which the complexified conductivity associated to the <math>U(1)</math> gauge symmetry is <math>\tau/2</math>.</p>
22.	<p><a href="#">Effect of Non-Linear Permittivity on Electric Field in Multi-layer Dielectrics in Cylindrical Geometry</a>  P Johri, CC Reddy - 14th Conference on Industrial and Information Systems, 2019</p> <p><b>Abstract:</b> When operating under alternating current fields, the capacitive effect of cable insulation takes precedence over the resistive effect and its permittivity assumes a higher importance compared to electrical conductivity towards the distribution of electric field. Research in the past has shown that relative permittivity of a dielectric has a dependence on operating temperature, electric field and frequency. In this paper, the authors present a study on the effect of temperature and field dependent, non-linear permittivity on the resultant radial electric field distribution in case of a multi-dielectric insulation system in a two-dimensional cylindrical geometry. The effects of permittivity coefficients, conductor boundary temperature and applied average electric field on the distribution and peak of resultant field have been investigated. The authors believe that these results will prove to be useful in selection of additional layers of insulation in multi-dielectric power cables and cable joints.</p>

[Effect of Parametric Uncertainties on Fracture Behavior of Cortical Bone using XIGA](#)  
A Soni, S Kumar, N Kumar - Engineering Fracture Mechanics, 2020

23. **Abstract:** Bone tissues are heterogeneous composites that consist of various microstructural constituents at different length scales. These microstructural constituents and their heterogeneous distribution significantly affect the fracture behavior of bones. Thus, the effect of parametric uncertainties on the fracture analysis of a cortical bone is presented in this study. A 2D model of the cortical bone is generated with the help of micro-CT image of a cortical bone and the fracture analysis is performed for the developed model with the help of an Extended Isogeometric Analysis (XIGA) using linear elastic fracture mechanics. The values of stress intensity factor are calculated with the help of interaction integral approach and the direction of crack propagation after each step is evaluated using the maximum principle stress criterion. The obtained results are compared with the finite element results using Abaqus software and found in good agreement. Further, uncertainties in the values of osteon Young's modulus, cement line thickness and porosity percentage are taken into consideration for stochastic analysis. The effect of variation in the values of input parameters on the stress intensity factor values and the crack path trajectories is illustrated, and observed that the variation in osteon Young's modulus and porosity percentage is more pronounced than the cement line thickness.

**Graphical Abstract:**



[Effect of Step Duration on Breakdown in Needle-Plane Geometry Under DC Step Voltages](#)  
AJ Thomas, CC Reddy - 4th International Conference on Condition Assessment Techniques in Electrical Systems 2019

24. **Abstract:** In this paper, dc electrical treeing breakdown experiments are conducted using needle-plane system. Electrical treeing test can be used for the assessment of life estimation of the insulating material by estimating the voltage endurance coefficient and accumulated damage. Damage equalization method (DEM) is used for estimating the life of the dielectric material used in HVDC cables. Breakdown experiments are conducted with progressive voltage steps of different step size. Interesting new results on the role of different step size on breakdown voltage is reported which in turn shows the effect of space charge injection and accumulation. The results from the space charge distribution in a plane-plane geometry justify the authors' results on the effect step size on dc breakdown in needle-plane geometry. The experimental results obtained are compared with data available in the literature for ac electrical treeing tests for different rate of progressive voltage rise.

[Elasto-Plastic Fracture Modeling for Crack Interaction with XFEM](#)

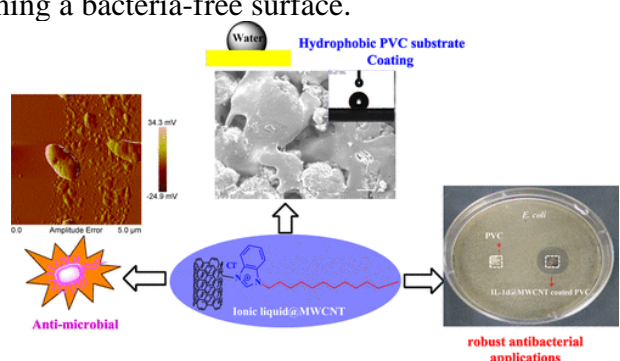
M Gajjar, H Pathak, S Kumar - Transactions of The Indian Institute of Metals, 2020 - Springer

25. **Abstract:** Multiple cracks/voids have been extensively seen in structural components. The stress field gets affected due to the crack interaction, so the effect of multiple cracks should be considered in design analysis. Further, due to service load, the stress concentrations are induced at the crack tips, which is the source of failure of the component. Hence, the current work has been proposed to investigate the crack interaction phenomenon in structural components under mechanical loading conditions. A mesh-independent computational approach, namely



	<p>“Extended Finite Element Method (XFEM),” has been implemented for crack discontinuities modeling. Ramberg–Osgood material model has been used for the nonlinear stress–strain relationship of material. Isotropic hardening has been used with von Mises yield criteria to decide the plasticity condition. Further, nonlinear discrete equations have been solved by the Newton–Raphson iterative scheme. Few crack interaction problems are numerically solved by the presented EPFM approach, and results are presented in the form of fracture parameters.</p>
26.	<p><a href="#">Enhanced Cavitation Erosion–Corrosion Resistance of High-Velocity Oxy-Fuel-Sprayed Ni-Cr-Al<sub>2</sub>O<sub>3</sub> Coatings Through Stationary Friction Processing</a>  HS Arora, M Rani, G Perumal, H Singh, HS Grewal - <i>Journal of Thermal Spray Technology</i>, 2020</p> <p><b>Abstract:</b> Cavitation erosion is a huge problem in engineering structures working under hydrodynamic conditions. The synergistic effect of erosion and corrosion can aggravate the material removal by several orders of magnitude. Surface coatings are widely used to address material degradation by erosion–corrosion. However, non-homogenous microstructure and presence of defects leads to premature coating failure under erosion–corrosion conditions. Thus, it is imperative to identify plausible solutions to address cavitation-related material degradation. In this study, Ni-Cr-5Al<sub>2</sub>O<sub>3</sub> coatings were deposited on stainless steel substrate using high-velocity-oxy-fuel technique. The as-sprayed coating showed highly non-homogeneous microstructure comprising splats, pores, intermetallic compounds and elemental segregation. A new thermo-mechanical processing technique, stationary friction processing (SFP), was utilized for achieving through-thickness microstructural refinement in as-sprayed coating. As-sprayed and SFP-treated coatings were tested in pure cavitation erosion, corrosion in 3.5% NaCl solution and erosion–corrosion. SFP treatment resulted in 5-times enhancement in the erosion and corrosion resistance compared to as-sprayed coating. The remarkable performance of Ni-Cr-5Al<sub>2</sub>O<sub>3</sub> coatings after SFP treatment is attributed to significant enhancement in the mechanical properties including hardness and fracture toughness which is the consequence of complete removal of splat boundaries, pores, intermetallic compounds and uniform element distribution up to the coating–substrate interface.</p>
27.	<p><a href="#">Estimation of Endurance Coefficient of Oil Impregnated Kraft Papers using DEM</a>  GN Reddy, B Singh, APS Tiwana, CC Reddy - <i>4th International Conference on Condition Assessment Techniques in Electrical Systems</i>, 2019</p> <p><b>Abstract:</b> Kraft paper is one of the most commonly used insulation in transformers and cables. Impregnation with transformer grade mineral oil is done to improve the electrical properties of the paper. Voltage endurance coefficient (n) is used to estimate the performance characteristics of the insulation paper aging. In this paper, a comparative study is done to estimate the endurance coefficient using conventional V-t curve method and Damage Equalization Method (DEM). The endurance coefficient is also known as the power law coefficient which is used in the V-t curve method to characterize the insulation aging. The unknown power law coefficient is also obtained from known values of step durations and stresses for each sample till its breakdown under DEM. Various types of AC Breakdown tests were performed on cable insulation of different ages obtained from a local manufacturer.</p>
28.	<p><a href="#">Experimental Analysis of a Novel Solar Pond Driven Thermoelectric Energy System</a>  R Goswami, R Das - <i>Journal of Energy Resources Technology</i>, 2020</p> <p><b>Abstract:</b> This paper describes an experimental study on a combined assembly of solar pond and two-phase thermosyphon towards thermoelectric power generation under actual weather conditions and proposes its mandatory association with biomass energy based system. Experiments under the studied solar radiation intensity ranging between 26 W/m<sup>2</sup>–976 W/m<sup>2</sup> reveal that the maximum steady-state temperature potential during the actual operation of a solar pond is not sufficient to generate the minimum threshold thermoelectric voltage for deriving necessary power needed to recharge a 12 V battery. It is also highlighted that solar radiation heats both the upper and the lower layers nearly equally, however, the heat is lost at a</p>

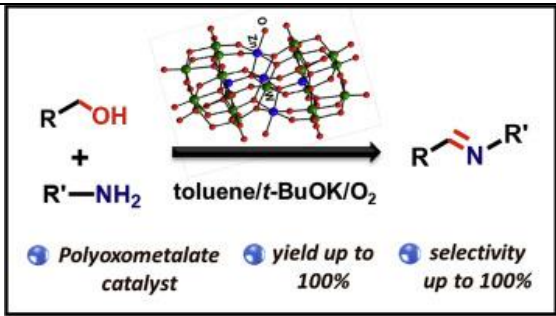
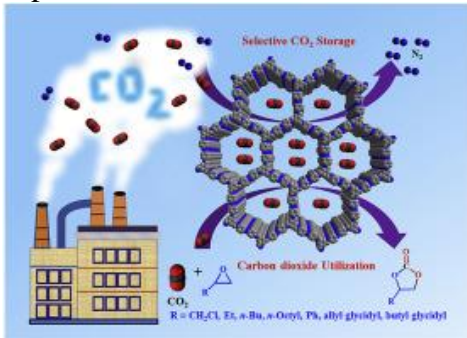
	<p>faster rate from the upper layer than the lower layer. Consequently, with the passage of time, the temperature of the lower layer rises, and interestingly the probability of obtaining maximum voltage during a day is maximum during the early morning. Under the present set of conditions, the maximum temperature gain is 26.58 °C, whereas, a minimum temperature potential of 45.62 °C is found necessary to produce the required voltage. Economic analysis of the proposed system reveals that the electricity generation obtained from the proposed system is better than diesel power generation. In particular, the system is suitable for locations where access to the conventional grid based power is difficult. The work opens opportunities and establishes the necessity of developing low cost thermoelectric materials for further improving the cost of power generation.</p>
29.	<p><a href="#">Experimental Investigation on Range of Fuel Premixing Ratio for Stable Engine Operation of Dual Fuel Engine Using Port Injection of Gasoline/Methanol and Direct Injection of Diesel</a> MR Saxena, RK Maurya - <i>Advances in Energy Research, Part of the Springer Proceedings in Energy book series</i>, 2020</p> <p><b>Abstract:</b> This study experimentally determines the range of fuel premixing ratio (PMR) for dual fuel compression ignition (CI) engine operated with a port injection of gasoline/methanol and direct injection of diesel. A stationary compression ignition engine (genset type) with a constant speed of 1500 rpm is used for the dual fuel experiments. The intake manifold of the engine was modified to run the engine in dual fuel mode. A port fuel injection controller was developed for injecting the required proportion of gasoline or methanol in the intake manifold. Experiments were performed for different fuel PMR at lower (25%), medium (50%) and high (100%) engine load conditions. The cycle-to-cycle variations in the combustion cycle and unburned HC (hydrocarbon) emissions are used for estimating the range of fuel PMR in dual fuel operation. The results revealed that the cyclic variation reduces with engine load for both the dual fuel operations, i.e., gasoline/diesel and methanol/diesel. Cyclic variations increase with higher fraction of gasoline/methanol in dual fuel operation. Results also demonstrate that higher cycle-to-cycle variations and unburned HC emissions limit fuel premixing range in dual fuel operation. The range of fuel premixing ratio is lower for methanol/diesel operation in comparison with gasoline/diesel dual fuel operation.</p>
30.	<p><a href="#">Formation and Decay of the Composite System <math>Z = 120</math> in Reactions with Heavy Ions at Energies Near the Coulomb Barrier</a> KV Novikov, EM Kozulin, GN Knyazheva, ...PP Singh...- <i>Bulletin of the Russian Academy of Sciences: Physics</i>, 2020</p> <p><b>Abstract:</b> The mass, energy and angular distributions of binary fragments formed in the reactions <math>^{64}\text{Ni} + ^{238}\text{U}</math>, <math>^{58}\text{Fe} + ^{244}\text{Pu}</math>, <math>^{52}\text{Cr} + ^{248}\text{Cm}</math>, <math>^{54}\text{Cr} + ^{248}\text{Cm}</math> at energies near the Coulomb barrier have been measured. The analysis of energy distributions of the symmetric fragments with mass numbers <math>ACN/2 \pm 20</math> <math>ACN/ACN22 \pm 20</math> formed in these reactions have been applied to separate compound nucleus fission and quasi-fission. The estimated fusion probability for the reactions Cr, Fe, and Ni ions with actinide targets shows an exponential dependence on the mean fissility parameter of the system and shows also that reaction with Cr ions is more favorable for production of the super heavy element with <math>Z = 120</math>.</p>
31.	<p><a href="#">GAZED—Gaze-guided Cinematic Editing of Wide-Angle Monocular Video Recordings</a> KLB Moorthy, M Kumar, R Subramanian, V Gandhi - <i>CHI Conference Paper</i>, 2020</p> <p><b>Abstract:</b> We present GAZED— eye GAZe-guided EDiting for videos captured by a solitary, static, wide-angle and high-resolution camera. Eye-gaze has been effectively employed in computational applications as a cue to capture interesting scene content; we employ gaze as a proxy to select shots for inclusion in the edited video. Given the original video, scene content and user eye-gaze tracks are combined to generate an edited video comprising cinematically valid actor shots and shot transitions to generate an aesthetic and vivid representation of the original narrative. We model cinematic video editing as an energy minimization problem over shot selection, whose constraints capture cinematographic editing conventions. Gazed scene</p>

	locations primarily determine the shots constituting the edited video. Effectiveness of GAZED against multiple competing methods is demonstrated via a psychophysical study involving 12 users and twelve performance videos.
32.	<p><a href="#">Impact of Harmonic Road Disturbances on Active Magnetic Bearing Supported Flywheel Energy Storage System in Electric Vehicles</a> T Soni, R Sodhi - IEEE Transportation Electrification Conference, 2019</p> <p><b>Abstract:</b> Flywheel Energy Storage System (FESS) are being considered as a promising solution for energy storage in Electric Vehicles (EVs). However, usage of conventional bearings for such high speed rotors will cause high noise level in the vehicle. On the other hand, Active Magnetic Bearings (AMBs) can offer contactless suspension for the flywheel rotor system, thereby, resulting in noiseless operation of the FESS. Owing to the irregular road conditions, the AMB-FESS system will be subject to parametric excitation, which is known to cause instability in a system. This work therefore tests the performance of AMBs for FESS, in the case of a EV subject to harmonic base pitch, roll and heave motion with different frequencies.</p>
33.	<p><a href="#">Ionic Liquid-Functionalized Multiwalled Carbon Nanotube-Based Hydrophobic Coatings for Robust Antibacterial Applications</a> D Bains, G Singh, J Bhinder, PK Agnihotri, N Singh - ACS Applied Bio Materials, 2020</p> <p><b>Abstract:</b> In recent years, the biomimetic superhydrophobic coatings have received tremendous attention, owing to their potential in fabricating self-cleaning surfaces, in environmental applications. Consequently, extensive research has been devoted to create a superhydrophobic surface using the oxidized derivatives of CNTs and graphene. Thus, the design and development of a self-cleaning/superhydrophobic surface with good biocompatibility are an effective approach to deal with the bacterial infections related to biomedical devices used in hospitals. In this context, herein, we have developed the material based on ionic liquid (IL)-functionalized multiwalled carbon nanotubes (MWCNTs) for hydrophobic coatings, which was fully characterized with various techniques such as Fourier transform infrared, powder X-ray diffraction, energy-dispersive X-ray spectroscopy, and scanning electron microscopy. We have evaluated the synthesized ILs for their antibacterial potential against the pathogenic bacterial strains such as Gram-positive (Staphylococcus aureus and methicillin-resistant S. aureus) and Gram-negative (Escherichia coli) bacterial strains. Further, atomic force and scanning electron microscopic studies have been performed to investigate the morphological changes to unravel the mechanism of action, whereas DNA binding study indicates the binding of IL-1d@MWCNT with DNA (<math>K_a = 2.390 \times 10^4 \text{ M}^{-1}</math>). Furthermore, the developed material (IL-1d@MWCNT) is coated onto the surface of polyvinyl chloride (PVC) and evaluated for hydrophobicity through water contact angle measurements and possesses long-term antibacterial efficiency against both under-investigating pathogenic strains. For the biocompatibility assay, the obtained coated PVC material has also been evaluated for its cytotoxicity, and results reveal no toxicity against viable cells. These all results are taken together, indicating that by coating with the developed material IL-1d@MWCNT, a robust self-sterilizing surface has achieved, which helps in maintaining a bacteria-free surface.</p> 

34.	<p><a href="#">Mapping of deflection caused due to hydrostatic pressure using Differential SAR Interferometry (DInSAR) on Bhakhra dam</a> A Tripathi, RK Tiwari - International Conference on Electrical, Electronics and Computer Engineering, 2019</p> <p><b>Abstract:</b> Microwave remote sensing is truly the most rapidly emerging field of satellite remote sensing today. In a very short span of time, it has found variety of applications in almost every field which had seen optical remote sensing dominance. This shows that its both state of the art and a versatile non-evasive remote sensing tool. It has added advantage of all-weather availability and penetration abilities which the optical remote sensing lacks. Hence can be easily used for areas and months with dense cloud cover. Of the many applications of SAR (Synthetic Aperture RADAR) or Microwave remote sensing is its ability to map and monitor land surface deformations shown by both natural and man-made features over a period, which helps as an early warning for many possible disastrous events like structural failures in dams. The technique involved is Differential SAR Interferometry or DInSAR. DInSAR involves a repeat pass configuration of SAR Interferometry with minimum baseline. The presence of any random motion on the surface or surface features on earth, tends to decorrelate the backscatter signals and add noise to phase difference. Small change due to surface movements, causes change in phase difference which is measured precisely and accurately by this technique. This study aims to measure the deflection that has come over a period of one year on the walls of Bhakhra Dam in Himachal Pradesh in India, due to the change in water levels and pressure exerted by it. Using DInSAR, the deflection was measured to be around 0.952cm from August 2017 to October 2017.</p>
35.	<p><a href="#">Multifunctional Receptor with Tunable Selectivity: A Comparative Recognition Profile of Organic Nanoparticles with Carbon Dots</a> G Kaur, H Kaur, A Singh, M Chaudhary, N Kaur, N Singh, KC Jena – Chemistry – An Asian Journal, 2020</p> <p><b>Abstract:</b> The exponential growth in the research field of water pollution control demands the evolution of novel sensing materials for regulation and quantification of metals ions. Within this context, the current work reports a new strategy for the synthesis of carbon dots from the hydrothermal treatment of organic nanoparticles. The organic nanoparticles are found to be selective towards Cs (I) ions with a detection limit of 5.3 nM, whereas the highly fluorescent carbon dots are found to be selective towards Ag (I) ions with detection limit of 4.8 nM. Both the sensing systems illustrate rapid sensing with working pH range from 4-9. The interfacial molecular restructuring of the sensing systems in aqueous phase has been investigated in the absence and presence of targeted metal ions using sum frequency generation vibrational spectroscopic tool. The practical applicability of the sensors was checked in environmental samples. This work opens new avenues for the exploration of temperature guided sensing modulation in nanomaterials.</p>
36.	<p><a href="#">Persistence and stability of interacting species in response to climate warming: The role of trophic structure</a> T Kaur, PS Dutta - Theoretical Ecology, 2020</p> <p><b>Abstract:</b> Over the past century, the Earth has experienced roughly 0.4–0.8 °C rise in the average temperature and which is projected to increase between 1.4 and 5.8 °C by the year 2100. The increase in the Earth's temperature directly influences physiological traits of individual species in ecosystems. However, the effect of these changes in community dynamics, so far, remains relatively unknown. Here, we show that the consequences of warming (i.e., increase in the global mean temperature) on the interacting species persistence or extinction are correlated with their trophic complexity and community structure. In particular, we investigate different nonlinear bioenergetic tri-trophic food web modules, commonly observed in nature, in the order of increasing trophic complexity: a food chain, a diamond food web, and an omnivorous interaction. We find that at low temperatures, warming can destabilize the species dynamics in the food chain as well as the diamond food web, but it has no such effect on the trophic structure</p>



	<p>that involves omnivory. In the diamond food web, our results indicate that warming does not support top-down control induced co-existence of intermediate species. However, in all the trophic structures, warming can destabilize species up to a threshold temperature. Beyond the threshold temperature, warming stabilizes species dynamics at the cost of the extinction of higher trophic species. We demonstrate the robustness of our results when a few system parameters are varied together with the temperature. Overall, our study suggests that variations in the trophic complexity of simple food web modules can influence the effects of climate warming on species dynamics.</p>
37.	<p><a href="#">Physical insights into principal component thermography</a> K Kaur, A Sharma, A Rani, V Kher, R Mulaveesala - <i>Insight-Non-Destructive Testing and Condition Monitoring</i>, 2020</p> <p><b>Abstract:</b> Among widely used non-destructive testing (NDT) methods, infrared thermography (IRT) has gained importance due to its fast, whole-field, remote and quantitative inspection capabilities for the evaluation of various materials. Being fast and easy to implement, pulsed thermography (PT) plays a vital role in the infrared thermographic community. This paper provides a physical insight into the selection of empirical orthogonal functions obtained from principal component pulsed thermography for the detection of subsurface defects located inside a mild steel specimen.</p>
38.	<p><a href="#">PMUs Enabled Tellegen's Theorem-Based Fault Identification Method for Unbalanced Active Distribution Network Using RTDS</a> Y Bansal, R Sodhi - <i>IEEE Systems Journal</i>, 2020</p> <p><b>Abstract:</b> The correct identification of the fault in the distribution systems can help in the healing process, system restoration, and thus lessen the duration of the outage. With the latest trend of penetrating the DG with the distribution network, the conventional fault identification (FI) methods become inappropriate for the promising active distribution network. Hence, the FI methods in the multisource, unbalanced, and weak distribution system is a challenge. In this article, the entire network is divided into the number of zones with each phase representing the two-port network. Further, the adjoint network matrices are formed for each of the two-port networks. The Tellegen's theorem based on adjoint circuit concept is then, used to identify the open-circuit section or the faulted node in the network using the input and output port information only. The voltage and current phasor information of the ports are acquired from the phasor measurement units based on the DFT. The methodology has been extensively verified on the IEEE-13 and IEEE-34 bus distribution systems integrated with the DGs, for all types of open and short circuit faults, with very encouraging results, with the real-time digital simulator.</p>
39.	<p><a href="#">Polyoxometalate catalyzed imine synthesis: Investigation of mechanistic pathways</a> SD Adhikary, D Mandal - <i>Tetrahedron</i>, 2020</p> <p><b>Abstract:</b> The syntheses of imines by oxidative coupling of primary alcohols and amines were achieved by using 2 mol% polyoxometalate (POM) <math>\text{Na}_{12}[\text{WZn}_3(\text{H}_2\text{O})_2(\text{ZnW}_9\text{O}_{34})_2]</math> (<math>\text{Zn}-\text{WZn}_3</math>) catalyst in the presence of <i>t</i>-BuOK and di-oxygen with excellent conversion (up to 100%) and selectivity (up to 100%). Non-noble metal-based POM catalyst in the presence of base represents a new reaction protocol for the selective synthesis of imine from both aromatic and aliphatic primary amines with functional group tolerance. Control experiment shows the formation of di-oxygen bind <math>\text{Zn}-\text{WZn}_3</math> activated species. The electron-density of POM is mostly situated on the surface oxygen atoms of <math>\text{W}-\text{O}-\text{W}</math> bonds which can engage the alcoholic OH group and helps for the imine selectivity in the second step of imine synthesis.</p> <p><b>Graphical Abstract:</b></p>

		
40.	<p><a href="#">Porous nitrogen-rich covalent organic framework for capture and conversion of CO<sub>2</sub> at atmospheric pressure conditions</a>  SS Dhankhar, CM Nagaraja - Microporous and Mesoporous Materials, 2020</p> <p><b>Abstract:</b>  A porous nitrogen-rich imine-linked covalent organic framework (COF1) has been synthesized by Schiff-base condensation reaction of 4,4'-azodianiline (AZO) and benzene-1, 3, 5-tricarboxaldehyde (BTA) under solvothermal conditions and characterized by various techniques. Owing to the presence of basic imine (-C=N) and -azo (-N=N) functionalized 1D channels, COF1 exhibits high affinity for CO<sub>2</sub> with high isosteric heat of adsorption (Q<sub>st</sub>) value of 32.3 kJ/mol. Further, the COF1 supported ZnBr<sub>2</sub> acts as an excellent recyclable catalyst for cycloaddition of CO<sub>2</sub> to epoxides resulting in cyclic carbonates with high yield and 100% selectivity under solvent-free mild conditions of 1 bar of CO<sub>2</sub>. Further, the coordination of Zn(II) to basic -C=N group was supported by XPS studies and theoretical calculations. Interestingly, COF1 shows excellent recyclability and can be recycled for several cycles without substantial loss of catalytic activity and structural rigidity. The high CO<sub>2</sub> affinity combined with excellent thermal stability and catalytic activity make COF1 a promising candidate material for efficient fixation of carbon dioxide.</p> <p><b>Graphical abstract:</b>  Design of a porous nitrogen-rich imine-linked covalent organic framework (COF1) for selective capture and conversion of CO<sub>2</sub> into cyclic carbonates under environmental-friendly solvent-free mild conditions of atmospheric pressure of CO<sub>2</sub> has been demonstrated.</p> 	
41.	<p><a href="#">Rotational de-excitations of C<sub>3</sub>H<sup>+</sup> (1Σ<sup>+</sup>) by collision with He: new ab initio potential energy surface and scattering calculations</a>  S Chhabra, TJ Dhillip Kumar - Monthly Notices of the Royal Astronomical Society, 2020</p> <p><b>Abstract:</b> Molecular ions play an important role in the astrochemistry of interstellar and circumstellar media. C<sub>3</sub>H<sup>+</sup> has been identified in the interstellar medium recently. A new potential energy surface of the C<sub>3</sub>H<sup>+</sup>-He van der Waals complex is computed using the ab initio explicitly correlated coupled cluster with the single, double and perturbative triple excitation [CCSD(T)-F12] method and the augmented correlation consistent polarized valence triple zeta (aug-cc-pVTZ) basis set. The potential presents a well of 174.6 cm<sup>-1</sup> in linear geometry towards the H end. Calculations of pure rotational excitation cross-sections of C<sub>3</sub>H<sup>+</sup> by He are carried out using the exact quantum mechanical close-coupling approach.</p>	

	<p>Cross-sections for transitions among the rotational levels of <math>C_3H^+</math> are computed for energies up to <math>600\text{ cm}^{-1}</math>. The cross-sections are used to obtain the collisional rate coefficients for temperatures <math>T \leq 100\text{ K}</math>. Along with laboratory experiments, the results obtained in this work may be very useful for astrophysical applications to understand hydrocarbon chemistry.</p>
42.	<p><a href="#">Space Charge and DC Fields of Multilayer Dielectrics in Plane-Parallel Geometry</a>  P Muppala, CC Reddy - 4th International Conference on Condition Assessment Techniques in Electrical Systems, 2019</p> <p><b>Abstract:</b> Space charge always assumes critical importance when it pertains electro-thermal problem of a dielectric subjected to dc stresses for dc cable insulation in particular. The significance of space charge only increases when multilayer dielectrics, cable joints in particular, are concerned. Interfacial polarization, complex electric field distribution and dynamic boundary temperatures greatly increase the probability of breakdown of a multilayer dielectric. Hence as an extension to the authors' previous works this paper focuses on computation of space charge and its effects related to electric field and temperature profiles of a multilayer dielectric. Poisson's equation along with Maxwell-Wagner interfacial polarization equation were used to obtain space charge distribution at different boundary temperatures and fields. Net charge accumulation in individual layers at different boundary temperatures and fields were determined.</p>
43.	<p><a href="#">Spectrally Selective and Highly Sensitive UV Photodetection with UV-A, C Band Specific Polarity Switching in Silver Plasmonic Nanoparticle Enhanced Gallium Oxide Thin-Film</a>  K Arora, DP Singh, P Fischer, M Kumar - Advanced Optical Materials, 2020</p> <p><b>Abstract:</b> Traditional photodetectors generally show a unipolar photocurrent response when illuminated with light of wavelength equal or shorter than the optical bandgap. Here, it is reported that a thin film of gallium oxide (GO) decorated with plasmonic nanoparticles, surprisingly, exhibits a change in the polarity of the photocurrent for different UV bands. Silver nanoparticles (Ag NPs) are vacuum-deposited onto <math>\beta\text{-Ga}_2\text{O}_3</math> and the AgNP@GO thin films show a record responsivity of <math>250\text{ A W}^{-1}</math>, which significantly outperforms bare GO planar photodetectors. The photoresponsivity reverses sign from <math>+157\text{ }\mu\text{A W}^{-1}</math> in the UV-C band under unbiased operation to <math>-353\text{ }\mu\text{A W}^{-1}</math> in the UV-A band. The current reversal is rationalized by considering the charge dynamics stemming from hot electrons generated when the incident light excites a local surface plasmon resonance in the Ag nanoparticles. The Ag nanoparticles improve the external quantum efficiency and detectivity by nearly one order of magnitude with high values of <math>1.2 \times 10^5</math> and <math>3.4 \times 10^{14}</math> Jones, respectively. This plasmon-enhanced solar blind GO detector allows UV regions to be spectrally distinguished, which is useful for the development of sensitive dynamic imaging photodetectors.</p>
44.	<p><a href="#">Sustainability in manufacturing processes: Finding the environmental impacts of friction stir processing of pure magnesium</a>  RK Sharma, GPS Sodhi, V Bhakar, R Kaur...P Sarkar, H Singh - CIRP Journal of Manufacturing Science and Technology, 2020</p> <p><b>Abstract:</b> Manufacturing activities consume a significant share of energy and natural resources and create some irreversible environmental impacts leading to climate change. A recent report from IPCC has highlighted the seriousness of global climate change. To mitigate the environmental burdens from manufacturing activities, it is necessary to identify and visualize them. Tools based on life cycle assessment (LCA) method have proven capabilities to visualize the hotspots during different stages of product life cycle and to support decision-making. This paper presents friction stir processing (FSP) of pure magnesium for bio implants and its environmental impact assessment in the Indian context. The study is aimed to visualize the FSP of pure Mg and major hotspots in the process to improve sustainability. The primary data for the inventory analysis was collected using real-time observations during each step of the process; whereas for secondary data, product catalogs and reports were utilized. The analysis shows that the production process of magnesium and energy used during electric discharge machining (EDM) have the highest environmental impacts. Additionally, in magnesium</p>

	<p>production, the direct emissions generated due to the burning of fossil fuel are the major contributors to these impacts. The steel used for FSP tool production and brass wire used in EDM for sizing of the magnesium plates, are also found to be contributing significantly toward water depletion potential. The study provides a conceptual approach including possible technological interventions to improve the process sustainability. The study suggests adopting advanced technologies of practical significance like ‘zinc coated cutting wires’ for improving the environmental performance of the process.</p>
45.	<p><a href="#">Temperature-Aware Closed-Form Matrix Rational Approximation Model for Crosstalk Analysis of Multi-Walled Carbon Nanotube Interconnects</a>  S Guglani, A Kumar, R Kumar...R Sharma... - <i>Electrical Design of Advanced Packaging and Systems</i>, 2019</p> <p><b>Abstract:</b> This paper presents a temperature-aware matrix rational approximation (MRA) technique for the predictive modeling of multiwall carbon nanotube (MWCNT) on-chip interconnect networks. The key feature of the proposed technique is its capacity to account for the effects of temperature variations on the crosstalk in MWCNT networks without having to reconstruct the model.</p>
46.	<p><a href="#">Testing deviations from PPP and UIP: evidence from BRICS economies</a>  KP Prabheesh, B Garg - <i>Studies in Economics and Finance</i>, 2020</p> <p><b>Abstract:</b>  Purpose  This paper aims to investigate the interrelations between purchasing power parity (PPP) and uncovered interest parity (UIP) in BRICS economies, namely, Brazil, Russia, India, China and South Africa, by checking the validity of the capital-enhanced equilibrium exchange rate (CHEER) approach. Further, this study tests whether the CHEER results are data frequency-dependent.  Design/methodology/approach  The present study uses monthly data ranging from 1997M01 to 2016M12 and considers the US economy as the representative foreign country. The study uses structural break unit root test and structural break cointegration technique to test the presence of economic relationships between nominal exchange rates and each of the price and interest rate differentials. Then, the study examines the validity of the CHEER approach by testing the appropriate theoretical restrictions.  Findings  The cointegration results suggest the existence of two cointegrating vectors representing UIP and PPP conditions. For all countries, the data appear to support the hypothesis that the system contains UIP and PPP relations. However, each of the international parity hypotheses is strongly rejected when formulated in isolation and jointly, leading to repudiation of the CHEER validity. Further, it is found that the results are data frequency-dependent and suggest that higher frequencies should be used as they provide additional information.  Originality/value  First, the literature on equilibrium exchange rates in BRICS economies is scanty. BRICS economies are large-emerging economies and one of the fastest growing economies and thus entail an empirical enquiry on their exchange rates. Second, the empirical application has mainly used monthly data to test the validity of the CHEER approach. However, data frequencies could affect the results. To the best of the authors’ knowledge, this study is the first to check data frequency-dependency in examination of the CHEER approach.</p>
47.	<p><a href="#">Testing the intertemporal sustainability of current account in the presence of endogenous structural breaks: Evidence from the top deficit countries</a>  B Garg, KP Prabheesh - <i>Economic Modelling</i>, 2020</p> <p><b>Abstract:</b> We examine the sustainability of the current account (CA) deficits among the top deficit countries occurring consistently in the period after the global financial crisis period. Hence, we chose four developed economies, namely, Australia, Canada, the UK, and the US,</p>



	<p>and three emerging market economies, namely, Brazil, India, and Turkey. The results indicate that information about structural breaks, occurring around the GFC period, improves the cointegration results significantly. We find that five out of the seven countries, except Australia and the UK, exhibit sustainable CA deficits. Further, results with disaggregated CA indicates that the services account is sustainable in all countries while goods account is unsustainable in Australia, the UK, and India. Overall, our findings reveal the possibility of aggregation bias in affecting the CA sustainability results. Thus, CA deficits are not necessarily bad for an economy if it can generate sufficiently large future net export surpluses to pay its current net foreign outstanding debt.</p>
48.	<p><a href="#">Thermal modeling of single discharge in prospect of tool wear compensation in <math>\mu</math>EDM</a>  R Nadda, CK Nirala - <i>The International Journal of Advanced Manufacturing Technology</i>, 2020</p> <p><b>Abstract:</b> Due to the non-isoenergetic nature of discharge pulses in resistance-capacitance (RC) based micro electrical discharge machining (<math>\mu</math>EDM), the volume of produced micro-crater by each pulse varies significantly. This fact has driven the researchers in this work to propose an electrothermal principle-based analytical model to approximate dimensional accuracies of such micro-craters. A finite element (FE) simulation considering Gaussian heat flux distribution of single discharge <math>\mu</math>EDM has been performed at significant input parameters such as discharge energy, capacitance, and open-circuit voltage and compared with analytical simulation results. Upon validation of these simulated results with experimental results, nominal dimensional inaccuracies of 2–11% for a wide range of input parameters have been noticed. This effectively predicted crater dimension from the workpiece can be incorporated in the proposed thermal modeling-based real-time tool wear monitoring and compensation system through a unique strategy, which is discussed at the end.</p>
49.	<p><a href="#">Thermal non-destructive testing and evaluation for subsurface slag detection: numerical modelling</a>  V Arora, R Mulaveesala, G Dua, A Sharma - <i>Insight-Non-Destructive Testing and Condition Monitoring</i>, 2020</p> <p><b>Abstract:</b> Among various non-destructive testing and evaluation (NDT&amp;E) methodologies, active infrared thermography (IRT) has emerged as a viable testing technique for the inspection of materials used in various industrial applications. In recent years, pulse compression favourable IRT techniques and the associated post-processing schemes have been proposed by various research groups to enhance the inspection capabilities of existing conventional techniques, as well as to make experimentation simple and more reliable. This paper exploits a novel complementary coded thermal wave imaging scheme for NDT&amp;E applications, along with the associated data processing method, to enhance the test resolution and sensitivity. The proposed scheme has been numerically modelled on a metallic sample in order to test its capabilities for subsurface defect detection and characterisation.</p>
50.	<p><a href="#">Towards the prediction of intergranular fatigue crack initiation in metals due to hydrogen</a>  A Arora, H Singh, DK Mahajan - <i>Materials Science and Engineering: A</i>, 2020</p> <p><b>Abstract:</b> Hydrogen deteriorates the fatigue behaviour of metals by attacking their microstructure in different ways. For better clarity about hydrogen-based degradation of metals, it is vital to identify the microstructural configurations that promote fatigue crack initiation (FCI) in the presence of hydrogen. Intergranular regions in polycrystalline metals are more prone to hydrogen attack due to the prevailing atomic structure, elastic anisotropy, and plastic inhomogeneities causing increased hydrogen accumulation in this region. In this work, FCI is studied in a model material nickel in the uncharged and hydrogen charged state during in-situ strain controlled low cycle fatigue (LCF) testing under a scanning electron microscope (SEM). Crack initiation sites are characterized by investigating the elastic modulus in the loading direction as well as the maximum Schmid factor of the crack neighbouring grains extracted through the electron backscattered diffraction (EBSD) data. The crack frequency for the uncharged and hydrogen charged specimens is then analyzed using the difference in the elastic</p>

	modulus ( $\Delta E$ ), the difference in the maximum Schmid factor ( $\Delta m$ ), and $\Delta E/\Delta m$ ratio between the crack neighbouring grains. The comparison shows that for the hydrogen charged specimens, intergranular FCI sites show high values of $\Delta E/\Delta m$ compared to the uncharged specimens. These findings provide a predictive model for hydrogen linked FCI in metals. In addition, the synergistic role of the Hydrogen Enhanced Local Plasticity (HELP) mediated Hydrogen Enhanced Decohesion (HEDE) mechanism responsible for FCI is also demonstrated.
51.	<p><a href="#">Zirconium Phosphate Catalyzed Transformations of Biomass Derived Furfural to Renewable Chemicals</a>  A Kumar, R Srivastava - ACS Sustainable Chemistry &amp; Engineering, 2020</p> <p><b>Abstract:</b> This study deals with the development of an economical, ZrPO<sub>4</sub> mediated, one-step catalytic transformations of biomass-derived furfural to synthetic intermediates that have the capability to replace the conventional petrochemicals derived synthetic building blocks. ZrPO<sub>4</sub> is prepared via a highly energy-efficient process at ambient temperature in the eco-friendly ethanol medium. ZrPO<sub>4</sub> exhibits excellent activity in the transformation of furfural to furfuryl alcohol via eco-friendly and safe, alcohol mediated transfer-hydrogenation protocol. Further, furfural is also efficiently converted to furfural derived dihydropyrimidinone and 2-(furan-2-ylmethylene)malononitrile via multi-component Biginelli and Knoevenagel condensation reactions, respectively. Moreover, other structurally homologous biomass-derived reactants such as 5-hydroxymethyl furfural and 2,5-diformyl furan are also compared under the optimized reaction conditions along with conventional petrochemical-derived reactants such as benzaldehyde and 1-heptenal. The high activity of ZrPO<sub>4</sub> is correlated with the acidity/basicity, pyridine FT-IR measurements, and reactants adsorption experiments. The catalyst exhibits no significant change in the activity even after five recycles. Non-noble metal-catalyzed economical and sustainable process for furfuryl alcohol production will certainly motivate chemists and researchers. One simple catalyst affording three functional renewable synthetic intermediates from furfural will attract significant attention to catalysis researchers and industrialists.</p>

**Disclaimer:** This publication digest may not contain all the papers published. Library has compiled the publication data as per the alerts received from Scopus and Google Scholar for the affiliation “Indian Institute of Technology Ropar” for the month of May 2020. The author(s) are requested to share their missing paper(s) details if any, for the inclusion in the next publication digest.